Organic Process Research & Development **2004**, *8*, 609−615

Optimal Operation of a Seeded Pharmaceutical Crystallization with Growth-Dependent Dispersion

Daniel B. Patience,*,‡ Philip C. Dell'Orco,‡ and James B. Rawlings*,†

Department of Chemical and Biological Engineering, University of Wisconsin, 1415 Engineering Drive, Madison, Wisconsin 53706, U.S.A., and GlaxoSmithKline, 709 Swedeland Road, P.O. Box 1539, King of Prussia, Pennsylvania 19406, U.S.A.

Abstract:

A cooling profile for a seeded pharmaceutical crystallization designed to achieve a desired mean crystal size is found by minimizing the batch operating time subject to a crystallization model. In many systems, optimizing a characteristic of the product crystal size density is the usual objective. This objective is not feasible for this system because growth-dependent dispersion occurs in the absence of secondary nucleation. Instead, the batch operating time is minimized, and the resulting characteristics of the crystal size density are then fixed by the operating policy. To prevent undesired secondary nucleation, both a cooling-rate constraint and a supersaturation constraint are investigated. The optimal policies are implemented and verified experimentally. The experimental measurements include solution concentration, slurry transmittance, and video microscopy. The video microscopy is used to determine the mean crystal size and standard deviation. These values are found to agree closely with the model predictions for the optimal operating policies. In addition to determining the optimal operating policies, this study is the first to use video images for monitoring crystal size density mean and standard deviation as part of crystallizer model validation.

Introduction

Recent advances in the pharmaceutical industry have created a large number of drug substances, most of which are complex organic materials requiring solution crystallization as a purification technique. The final form of the crystal usually has more than one polymorph due to the complex nature of the organic molecule. As a consequence, once the drug substance is registered and approved, the production of the desired polymorph with desired size, habit, and morphology must be guaranteed. In most cases, seeding with the required polymorph and suppressing secondary nucleation produces a final product with the same polymorph as that of the seeds. Secondary nucleation of undesirable polymorphs is avoided by growing the seeds in metastable solutions.[1] However, the crystallization of the seeds does not always lead to a product with maximum stability and bioavailability. Usually the crystal with the greatest bioavailability is the one with the highest solubility. Sometimes the crystal with the greatest stability is the one with the lowest solubility.[2] Therefore, it is crucial to design a cooling and seeding protocol to maximize the bioavailability and stability of the final population of crystals. Traditionally, cooling profiles and seeding-load protocols have been optimized by experimentally investigating, through factorial designs, the effects of various operating parameters on the crystal product's yield.[3,4] Although the factorial design method can provide a solution to a design objective, the disadvantage is that the approach is not model-based. The resulting optimal experimental design is limited to implementation only on the equipment used for collecting the data, making scale-up difficult.

An alternative method for optimizing a seeded batch crystallization is to develop mathematical models to predict the solution concentration, crystal size, and yield as a function of the operating conditions and cooling profile. Modeling crystallization systems is well-established.[5,6] The general statement of the open-loop optimal operation is given by Miller and Rawlings.[7] Temperature is the manipulated variable, which is parametrized as piecewise linear in time. Matthews et al.[8] compute the influence of model parameter uncertainty on the cooling profiles. The authors set temperature constraints in which cooling within these constraints achieves a local optimal result. Matthews and Rawlings[9] study the effects of seed mass and profile duration on the final-time value of the mass of nuclei to mass of seeds. The authors find that increasing the seed load improves the filtration performance of the final product. However, optimizing the seed load requires knowledge of solid−liquid

* Authors for correspondence. (D.B.P.) Telephone: (610) 270-6743. E-mail: daniel.b.patience@gsk.com. (J.B.R.) Telephone: (608) 263-5859. Fax: (608) 265-8794. E-mail: jbraw@bevo.che.wisc.edu.

† University of Wisconsin.

‡ GlaxoSmithKline.

(1) Beckmann, W. Seeding the Desired Polymorph: Background, Possibilities, Limitations and Case Studies. *Org. Process Res. Dev.* **2000**, *4*, 372−383.

(2) Spruijtenburg, R. Examples of the Selective Preparation of a Desired Crystal Modification by an Appropriate Choice of Operating Parameters. *Org. Process Res. Dev.* **2000**, *4*, 403−406.

(3) Togkalidou, T.; Braatz, R. D.; Johnson, B. K.; Davidson, O.; Andrews, A. Experimental Design and Inferential Modeling in Pharmaceutical Crystallization. *AIChE J.* **2001**, *47*, 160−168.

(4) Owen, M. R.; Luscombe, C.; Lai, L. W.; Godbert, S.; Crookes, D. L.; Emiabata-Smith, D. Efficiency by Design: Optimisation in Process Research. *Org. Process Res. Dev.* **2001**, *5*, 308−323.

(5) Rawlings, J. B.; Miller, S. M.; Witkowski, W. R. Model Identification Control of Solution Crystallization Processes: A Review. *Ind. Eng. Chem. Res.* **1993**, *32*, 1275−1296.

(6) Winn, D.; Doherty, M. F. Modeling Crystal Shapes of Organic Materials Grown from Solution. *AIChE J.* **2000**, *46*, 1348−1367.

(7) Miller, S. M.; Rawlings, J. B. Model Identification Control Strategies for Batch Cooling Crystallizers. *AIChE J.* **1994**, *40*, 1312−1327.

(8) Matthews, H. B.; Miller, S. M.; Rawlings, J. B. Model Identification for Crystallization: Theory and Experimental Verification. *Powder Technol.* **1996**, *88*, 227−235.

(9) Matthews, H. B.; Rawlings, J. B. Batch Crystallization of a Photochemical: Modeling, Control and Filtration. *AIChE J.* **1998**, *44*, 1119−1127.

10.1021/op0340917 CCC: $27.50
Published on Web 06/12/2004

performance versus yield. Chung et al.[10] study the effect of including parameters of the seed size density with the temperature as manipulated variables. Chung et al.[10] show that optimizing over the seed size density has a larger effect on the product crystal size density than optimizing over the temperature profile. These modeling and experimental design techniques have been successfully applied to a wide range of organic systems,[11] and other systems such as biological,[12] enzymatic,[13] and polymerization systems.[14] The typical objectives for model-based experimental designs include minimizing the mass of nucleated to seed crystals, maximizing the mass of nucleated to seed crystals, minimizing the coefficient of variation of the product crystal size density (defined as the ratio of the crystal size density standard deviation to the crystal size density mean), and maximizing the yield.

Recently, we developed a model that describes growth for a seeded pharmaceutical crystallization with growth-dependent dispersion and no secondary nucleation.[15] The model predicts the time varying, solution concentration, slurry transmittance, crystal size density mean, and crystal size density standard deviation. The pharmaceutical system with growth-dependent dispersion and no secondary nucleation is interesting because the above-mentioned objectives for a typical model-based experimental design cannot be used once a final mean size or yield constraint is imposed. Instead, we describe alternative designs minimizing the batch time as well as present experimental data to validate the model predictions.

Experimental Apparatus

The experimental apparatus and measurements used in this study are described by Patience.[15] The crystallizer is a 2.2-L glass jacketed vessel. The temperature of the crystallizer is controlled by a model predictive controller. For a crystallization experiment, 63.6 g of pharmaceutical is dissolved in 1753.1 g of an alcohol solvent ($T^{sat} = 50.9$ °C) at a temperature of 60 °C. The solution is held at this temperature for 60 min, then cooled at 10 °C·h^{-1} to 50 °C and held for 30 min. For runs 18 and 20, the solution is then cooled at 10 °C·h^{-1}. At 49.1 °C, 0.5 mL of a pharmaceutical seed solution (8.4 mg seeds in 3.0 mL of an alcohol solvent) are injected into the crystallizer. The seeding point is designed to occur at supersaturation 0.07. The temperature profiles (explained in the Best Operating Policies section) after seeding are shown in Figure 1. The temperature range is kept small to reduce clogging of the densitometer filter and to provide a solution-phase concentration measurement. Low solids densities result during the crystallization. Low solids densities do not commonly occur in the pharmaceutical industry.

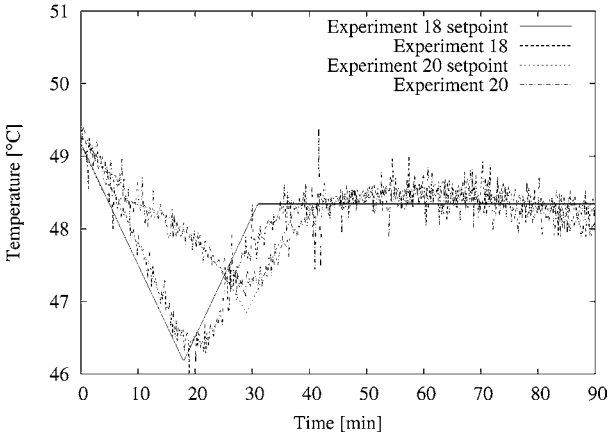

Figure 1. **Temperature profiles for runs 18 and 20.**

Photomicroscopy and digital image analysis are used to monitor growth kinetics and particle size characteristics of crystals in the size range of 10−1000 μm using an Olympus BX60 microscope, a Hitachi HV-C20 charged coupled device (CCD) camera and a PC with frame grabber and Image Pro Plus image analysis software. The microscope uses a nonpolarized reflected halogen light source with a total magnification of 8×. Samples of 0.5 mL of the crystal slurry are periodically removed from the crystallizer and placed under the microscope for image capture. The CCD camera captures images of 585 × 700 pixels with 256 grayness levels. The particles are then manually traced, and a pixel calibration is applied. For monitoring particle size, video-microscopy has advantages over the commonly used laser light-scattering techniques such as focused beam reflectance measurement (FBRM). For example, video-microscopy detects particle growth in two dimensions. Video-microscopy distinguishes between dissolution and agglomeration mechanisms during decreasing particle number counts. FBRM provides chord length measurements at a faster sampling rate than video-microscopy. However, when inverting signals from light-scattering patterns to obtain particle size, difficulties arise as the inversion problem is ill conditioned.[16,17]

On-line measurements of slurry temperature, slurry transmittance, and solution concentration are recorded. Temperature measurements are provided by in situ RTD thermocouples (accuracy ±0.2 °C). Transmittance measurements are provided by a Brinkman in situ colorimeter probe that is inserted into the headplate of the crystallizer and into the slurry. Incident light is transmitted from the colorimeter to the probe and passes through a 2-mm gap and is reflected back to the colorimeter sensor. Some light is scattered by

(10) Chung, S. H.; Ma, D. L.; Braatz, R. D. Optimal Seeding in Batch Crystallization. *Can. J. Chem. Eng.* **1999**, *77*, 590−596.
(11) Lang, Y.-D.; Cervantes, A. M.; Biegler, L. T. Dynamic Optimization of a Batch Cooling Crystallization Process. *Ind. Eng. Chem. Res.* **1999**, *38*, 1469−1477.
(12) Karlsson, J. O. M.; Eroglu, A.; Toth, T. L.; Cravalho, E. G.; Toner, M. Rational Design and Theoretical Optimization of a Cryopreservation Protocol. In *Advances in Heat and Mass Transfer in Biotechnology. American Society of Mechanical Engineers. HTD-Vol. 322/BED-Vol. 32* **1995**, 85−89.
(13) Faqir, N. M.; Attarakih, M. M. Optimal Temperature Policy for Immobilized Enzyme Packed Bed Reactor Performing Reversible Michaelis−Menten Kinetics Using the Disjoint Policy. *Biotechnol. Bioeng.* **2002**, *77*, 163−173.
(14) Gentric, C.; Pla, F.; Latifi, M. A.; Corriou, J. P. Optimization Nonlinear Control of a Batch Emulsion Polymerization Reactor. *Chem. Eng. J.* **1999**, *75*, 31−46.
(15) Patience, D. B. *Crystal Engineering Through Particle Size and Shape Monitoring, Modeling, and Control* (http://www.che.wisc.edu/jbr-group/theses/patience.pdf). Ph.D. Thesis, University of Wisconsin-Madison, 2002.
(16) Ruf, A.; Worlitschek, J.; Mazzotti, M. Modeling and Experimental Analysis of PSD Measurements Through FBRM. *Particle and Particle Systems Characterization* **2000**, *17*, 167−179.
(17) Miller, S. M. *Modelling and Quality Control Strategies for Batch Cooling Crystallizers* (http://www.che.wisc.edu/jbr-group/theses/miller.ps). Ph.D. Thesis, The University of Texas at Austin, 1993.

the crystal slurry. The ratio of transmitted to reflected light is recorded at 1-s intervals during the experiment (accuracy ±0.2%). Transmittance provides a measurement of the total projected surface area of all the crystals/particles. However, transmittance is limited to low solids densities and cannot distinguish between growth and nucleation events. A solids-free stream exits the crystallizer and passes through a Paar densitometer and then returns to the crystallizer at the same temperature as that of the crystallizer. The densitometer measures the solution-phase concentration at 20−30-s intervals (accuracy ±0.0002 g·g^{-1}). ATR-FTIR spectroscopy is an alternative measurement technique for solution-phase concentration and, unlike densitometry, is not limited to binary systems. ATR-FTIR spectroscopy is becoming widely used in the pharmaceutical industry for on-line concentration measurements because of the ease of use, high precision, and high sampling rate. The technique requires identification of detectable bond groups in the monitored molecule that will be detected in the IR spectra throughout the crystallization. The measurement deviates from the true solution concentration as systems become dilute. The solubility data used in this study are described by Patience.[15]

Isothermal Seed Growth Time

It is common in industry to operate a batch crystallizer at the end temperature until a low supersaturation is reached. To obtain the maximum yield, the crystallization model is used to estimate how long the end temperature should be kept constant. For a batch cooling crystallization, a zero supersaturation is never achieved unless the process is heated to zero supersaturation. Supersaturation is given as

$$S = \left(\frac{\hat{C} - \hat{C}_{\text{sat}}(T(t))}{\hat{C}_{\text{sat}}(T(t))} \right) \tag{1}$$

in which $\hat{C}$ is the solution-phase concentration and $\hat{C}_{\text{sat}}$ is the saturation concentration.

The batch crystallization model can be used to determine how long the operator must wait before close to zero supersaturation is achieved. Figure 2 shows the time to desupersaturate the isothermal solution at 49 °C as a function of the seed mass. Care must be taken when choosing the supersaturation threshold while calculating the desupersaturation time. A threshold supersaturation of 10^{-3} results in a desupersaturation time of 90 min to achieve a final mean size of 110 μm; however, for a supersaturation of 10^{-5}, 145 min are required to desupersaturate the solution. Figure 2 shows asymptotic behavior for desupersaturation time.

Best Operating Policies

It is desirable to manufacture crystals within a specified size range to avoid post-crystallization stages such as milling and sieving. For this pharmaceutical, we require the final product size range to be 20−200 μm, although this does not imply 200 μm is a size small enough to avoid milling in general. To maximize the mass of final product within the size range 20−200 μm, one possible objective is to minimize the coefficient of variation of the product crystal size density, with the mean constrained to the middle of the desired range. However, for a seeded crystallization with growth-dependent

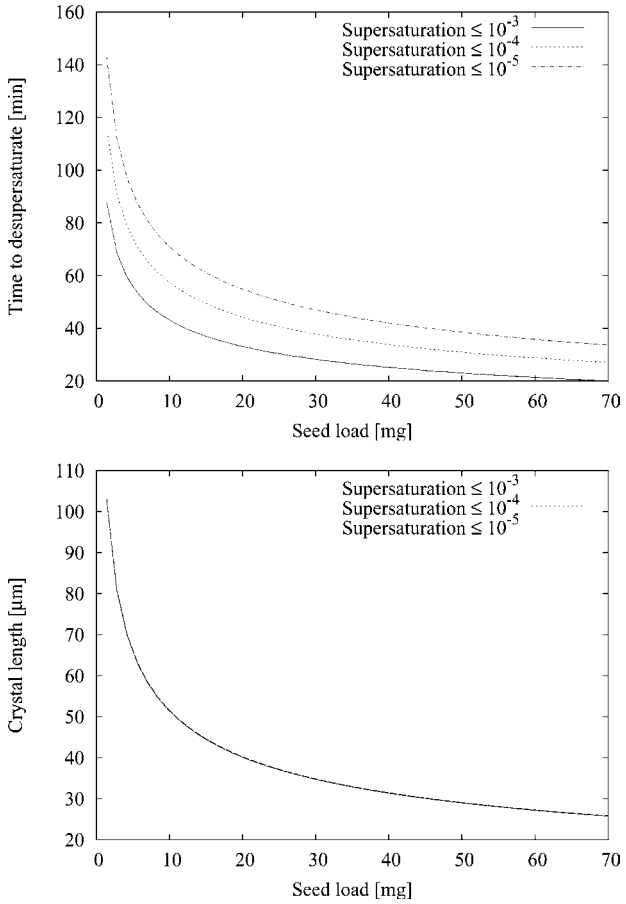

Figure 2. **Isothermal seed growth time. The time to desupersaturate the solution after seeding and the resulting mean crystal length as a function of seed loading.**

dispersion and no secondary nucleation, minimizing the coefficient of variation with a final mean size constraint is an *over-specified* problem. Given the initial seed crystal size density, any cooling profile that is implemented to take the process to the final required mean size always produces a crystal size density with the same coefficient of variation. There is no minimum coefficient of variation for this class of problems. Gentric et al.[14] study an analogous problem with a batch polymer reactor.

The model for crystallization with growth-dependent dispersion and the estimated parameters for the pharmaceutical system are presented by Patience.[15] Further model development for crystallization with growth-dependent dispersion is discussed by Kashchiev[18] and McCoy.[19] We assume secondary nucleation does not occur because of the small supersaturations studied, verified by photomicrograph images.[15] The kinetic expression for growth, G, is taken to be an empirical power law in supersaturation, S, given as

$$G = k_g S^g = k_g \left(\frac{\hat{C} - \hat{C}_{\text{sat}}(T(t))}{\hat{C}_{\text{sat}}(T(t))} \right)^g \tag{2}$$

(18) Kashchiev, D. *Nucleation*, 1st ed.; Butterworth-Heinemann: Oxford, England, 2000.
(19) McCoy, B. J. A New Population Balance Model for Crystal Size Distributions: Reversible, Size-Dependent Growth and Dissolution. *J. Colloid Interface Sci.* **2001**, *240*, 139−149.

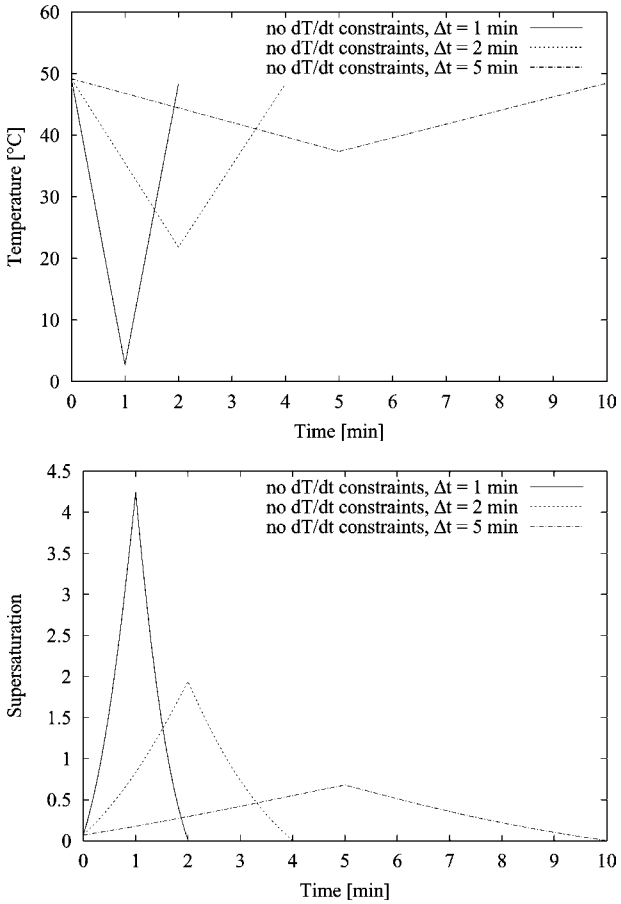

Figure 3. **Temperature and supersaturation profiles for batch crystallization. The profiles illustrated are for minimizing batch time with the final mean size constraint of 110 μm without constraints on the cooling rate and with the supersaturation constrained to be positive.**

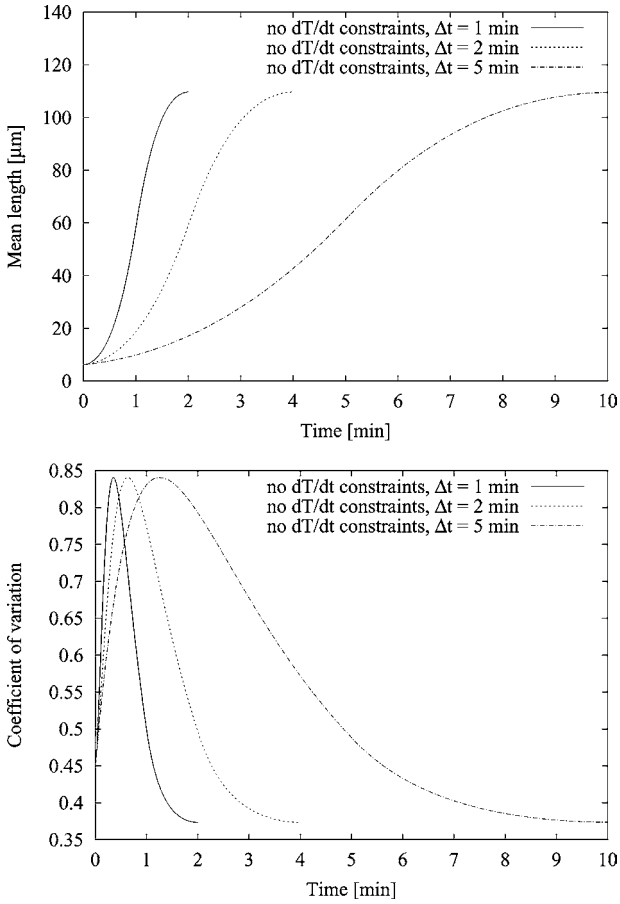

Figure 4. **Crystal mean length and coefficient of variation profiles for batch crystallization. The profiles illustrated are for minimizing batch time with the final mean size constraint of 110 μm without constraints on the cooling rate and with the supersaturation constrained to be positive.**

in which k_g is the growth rate constant and g the growth order. The seed crystal size density is assumed quadratic with a minimum size zero, and a maximum size of 12 μm.

The expression for growth-dependent dispersion, D, is the product of the growth rate and half the size of the growth unit, Δ, given as

$$D = G\frac{\Delta}{2} \tag{3}$$

The crystallization model describes crystal growth occurring in discrete sizes, Δ. In this study, Δ is approximately 9 μm. Dispersion is a natural consequence of the growth process and has a detrimental effect on the crystal size density. Provided there is a driving force for growth, the crystal size density continues to widen until supersaturation is zero, making the formation of a narrow crystal size density difficult. The effects from eqs 2 and 3 simultaneously decrease the solution concentration; however, the effects of dispersion must be minimized while maximizing the effects of growth.

The formulation of the optimal cooling profile problem is stated as the following: minimize the batch operating time, t_f, over the temperatures T_1, T_2, ..., T_N that are piecewise linear at the N points in time up to t_f. The problem is subject to the crystallization model and model parameters, initial conditions, terminal mean size of 110 μm, and final supersaturation equal to zero. The solution to this problem is readily computed using standard algorithms and software packages.[20] In this study, the optimal cooling profile problem is solved using a sequential quadratic program algorithm by implementing the NPSOL code.[21]

An example of minimizing the batch operating time while growing the seed crystals to the final mean size of 110 μm is given in Figures 3 and 4. Figures 3 and 4 show the influence of the element size, Δt, over which the optimization problem is solved. Care must be taken in interpreting the solution to this minimum batch time problem. For the simple case in which no temperature cooling- and heating-rate constraints are imposed, with a positive supersaturation throughout the run and supersaturation zero at the end of the run, the solution to the minimum batch time problem is $2\Delta t$. The profiles in Figures 3 and 4 are trivial solutions to the minimum batch time process. Given a finite number of seeds and a final required mean size, the solute mass required to be removed from solution and thus yield are specified.

(20) Moré, J. J.; Wright, S. J. *Optimization Software Guide*; SIAM: Philadelphia, 1993.

(21) Gill, P. E.; Murray, W.; Saunders, M. A.; Wright, M. H. *User's guide for SOL/NPSOL*, version 4.0; A Fortran package for nonlinear programming, technical report SOL 86-2. Technical report, Systems Optimization Laboratory, Department of Operations Research, Stanford University, 1986.

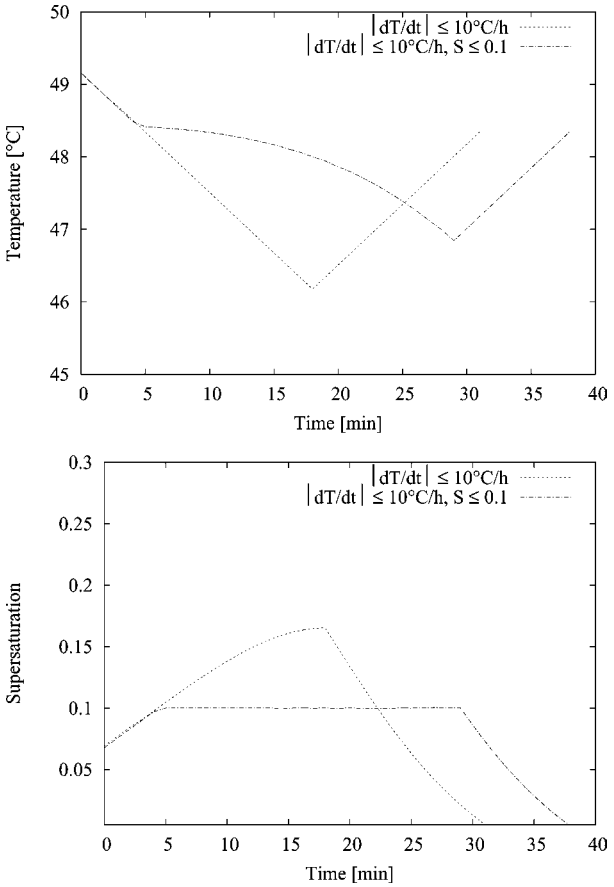

Figure 5. **Temperature and supersaturation profiles for batch crystallization. The profiles illustrated are for minimizing batch time with the final mean size constraint of 110 μm. Profiles are for cooling/heating rate dT/dt $\leq$ 10°C·h^{-1} and for dT/dt $\leq$ 10 °C·h^{-1} with a supersaturation constraint, $S \leq 0.1$ for Δt of 1 min.**

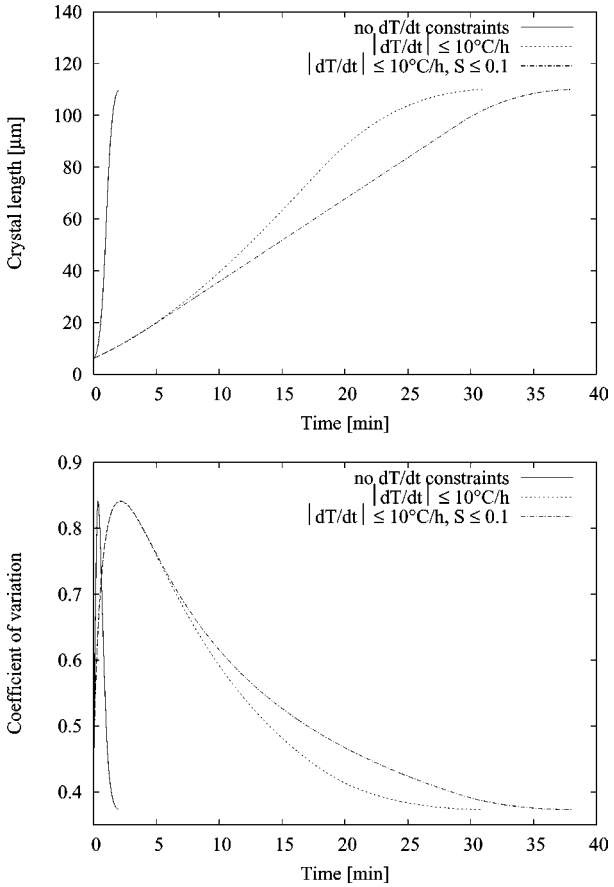

Figure 6. **Crystal mean length and coefficient of variation profiles for batch crystallization. The profiles illustrated are for minimizing batch time with the final mean size constraint of 110 μm. Profiles are for no cooling/heating rate, dT/dt constraints, dT/dt $\leq$ 10 °C·h^{-1}, and for dT/dt $\leq$ 10 °C·h^{-1} with a supersaturation constraint, $S \leq 0.1$, compared with the solution without constraints for Δt of 1 min.**

The first decision variable in the solution to the optimal cooling profile problem is a temperature in which almost half the mass of required solute will come out of solution in the first time step. The second and final decision variable is the temperature required to bring the supersaturation back to zero and remove the remaining required amount of solute from solution to achieve the final crystal size constraint. In the limit, as the time step, Δt, approaches zero, the response for supersaturation from the solution of the optimal cooling profile problem is a Dirac-δ function with area equal to the area under the supersaturation curve in Figure 3. Figure 4 shows that, once the mean size of the crystal size density has reached 110 μm, the coefficient of variation is the same for all the profiles. Care must be taken in not choosing Δt to be larger than half the total time interval when solving the optimal cooling profile problem. No solution to the optimal cooling profile problem exists once Δt becomes larger than half the total time interval for the given constraints.

The cooling profiles in Figure 3 are almost impossible to implement. The supersaturations are large, and secondary nucleation occurs for supersaturations greater than 0.2; thus, the model predictions in Figure 4 are invalid.[15] We first add a cooling constraint to make the problem more realistic. Figures 5 and 6 show the solution to minimizing batch time while imposing a cooling-rate constraint less than 10 °C·h^{-1}. The supersaturation for the cooling-rate constrained profile is never greater than 0.2 for this experiment. To demonstrate the influence of a supersaturation constraint on the cooling profile, we chose a supersaturation constraint less than or equal to 0.1. Figures 5 and 6 show the solution to minimizing batch time while imposing a cooling rate less than 10 °C·h^{-1} and a supersaturation constraint less than or equal to 0.1. The case in which no cooling-rate constraints are imposed for a time step of 1 min (from Figures 3 and 4) is also shown for comparison. The solution for the minimum batch time for the cooling-rate constrained profile is 31 min. For the supersaturation constraint less than or equal to 0.1, the minimum batch time to achieve the same size is 38 min. In the supersaturation-constrained case, the cooling profile is identical for the first 4 minutes, after which the supersaturation constraint becomes active. At this point the cooling rate decreases enough to avoid violating the supersaturation constraint. The temperature continues to cool, drawing out enough mass to grow the crystals to the desired size. Once almost enough mass has been withdrawn from solution to achieve the final size, the temperature increases at a rate equal to the constraint and heats the reactor to zero supersaturation at the point in which the crystal mean size is 110 μm.

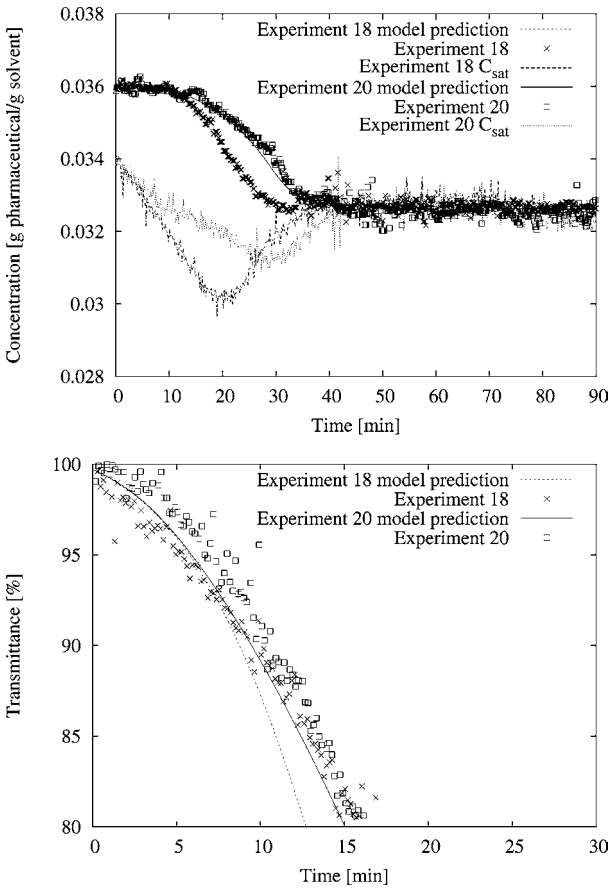

Figure 7. **Concentration and temperature experimental data for temperature-rate constrained and supersaturation-constrained experiments with model predictions.**

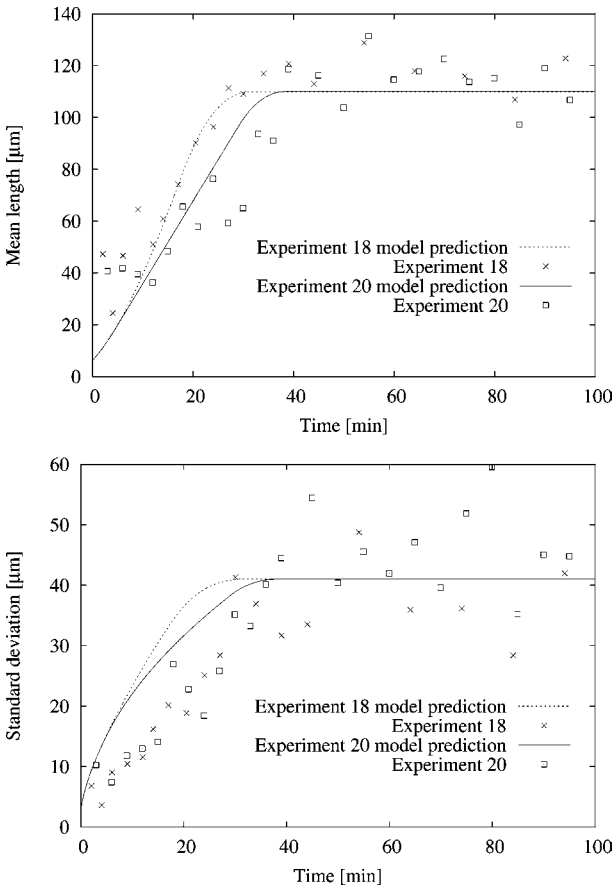

Figure 8. **Mean length and standard deviation experimental data for temperature-rate constrained and supersaturation-constrained experiments with model predictions based on 50−400 crystals per image/measurement.**

We implement the two operating policies for the cooling-rate constrained case (run 18) and the supersaturation constrained case (run 20). The concentration and transmittance data with predictions based on the identified model and estimated parameters in the study by Patience[15] for the experimental design are shown in Figure 7. The crystal size density mean and crystal size density standard deviation data with predictions are shown in Figure 8. The concentration data are relatively close to the concentration predictions except for some large short-time fluctuations caused by sensor noise. The transmittance readings do not closely follow the predictions; however, the transmittance response for run 20 is mostly slower than run 18 as predicted. The crystal size density mean and crystal size density standard deviation data agree within measurement error with the model predictions. In run 20, we detect a lower growth rate than run 18, as expected. The standard deviation data are not expected to agree well with the predictions because of the difficulty with varying sample sizes in photomicroscope images. Given the amount of noise in the crystal size data, we are able to achieve the required mean size within 10 μm.

Figure 9 shows the effects of increased seed load on the solution to the minimum batch crystallization time problem while having the cooling-rate constraint of 10 °C·h^{-1} and the final mean size of 110 μm. For the same value of the maximum seed size parameter, increased seed loads result in longer cooling times and shorter heating times. For largeenough seed loads, the optimizer has difficulty in finding the heating period to achieve zero supersaturation. The solution to the minimum batch time problem results in no heating unless the size of the time element over which the problem is solved is decreased. Figure 9 shows the cooling profile for a seed load of 1.4 mg and a maximum seed size of 6.2 μm. The crystallizer is cooled to 14 °C at 10 °C·h^{-1} for 210 min, after which a mean size of 110 μm is achieved. The extremely low temperature is required for this case because these seeds have a larger surface area per unit volume than the other runs so that they deplete the available supersaturation rapidly. However, due to their small initial size, the seeds must remain in the crystallizer for a long period to eventually grow to the desired size.

Increased seed loads can, of course, be used to increase the final yield if required. However, designing experiments with increased yield for a minimal operating time to achieve a final size constraint would require model identification of experiments outside of the temperature range and seed load studied. For simulation purposes, we demonstrate results for a low solids density process using the identified model obtained from the studied temperature range. Figure 10 shows the supersaturation and mean crystal length profiles for a process that is saturated at 70 °C and cooled to 0 °C at a cooling rate of 10 °C·h^{-1}. For the identical seed load used

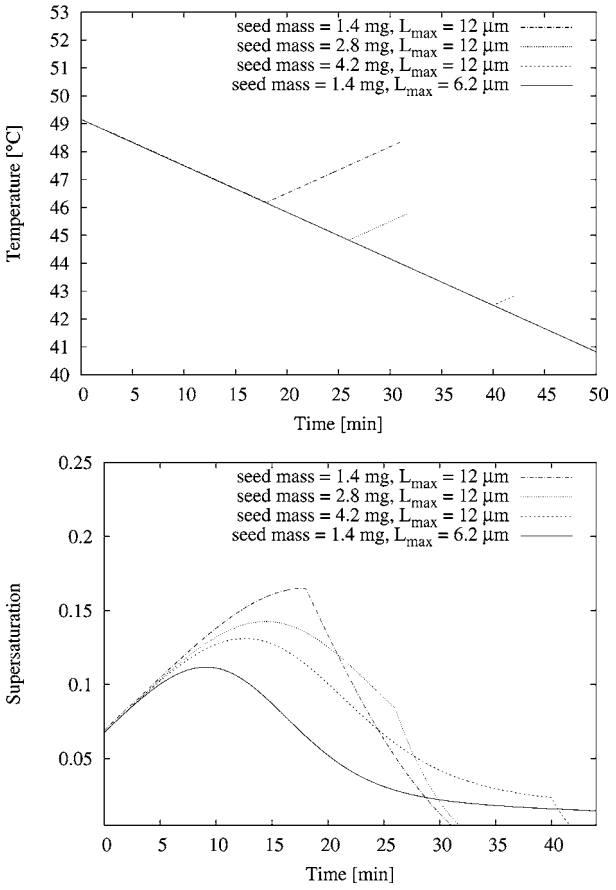

Figure 9. **Temperature and supersaturation profiles for batch crystallization. The profiles illustrated are for minimizing batch time as a function of initial seed loading and initial seed size, L_{max}. The final mean size constraint of 110 μm and a cooling-/heating-rate constraint $dT/dt \leq 10$ °C·h^{-1} are imposed.**

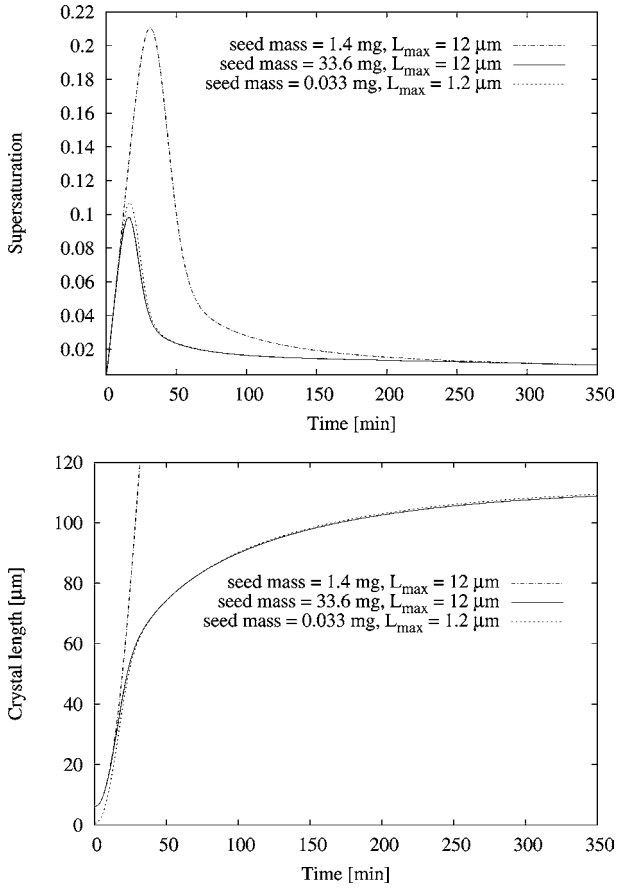

Figure 10. **Supersaturation and crystal mean size profiles for batch crystallization as a function of seed load and the maximum seed size. The profiles result from cooling a saturated solution from 70 to 0 °C at 10 °C·h^{-1}.**

in this study, the seeds grow to a mean size of 330 μm for the conditions. The seed loads required to produce the final mean size of 110 μm are calculated for the cases in which the maximum seed sizes are 12 and 1.2 μm. Figure 10 shows that a 10-fold decrease in the estimate for the maximum seed size leads to a 1000-fold decrease in the calculated seed load required to achieve the final size objective. Figure 10 shows that it is essential to have a narrow confidence interval on the maximum seed size parameter.

Conclusions

We have demonstrated model-based optimal operating procedures for a seeded pharmaceutical crystallization. For the particular class of seeded batch crystallization with growth-dependent dispersion and without secondary nucleation, it is impossible to change the crystal size density given a constraint on a final mean size. Instead, an appropriate objective is to minimize batch operating time subject to a final crystal size density mean size. The effects of cooling-rate and supersaturation constraints on the minimal operating time are investigated for the pharmaceutical crystallization. The solution to minimum batch operating time for a pharmaceutical crystallization results in a cooling profile equal to the cooling- and heating-rate constraints. If the supersaturation constraint is violated by this cooling pro file, then the solution to the minimum batch operating time problem is a cooling profile that generates a supersaturation equal to the supersaturation constraint. The optimal operating policy to achieve a user-specified mean crystal size is implemented, and the concentration and crystal size density mean size predictions are found to agree closely with the data. We also demonstrate a new use of video images for monitoring the crystal size density mean and crystal size density standard deviation as a means for model validation.

Acknowledgment

We gratefully acknowledge the financial support of GlaxoSmithKline. We also gratefully acknowledge the financial support of the industrial members of the Texas-Wisconsin Modeling and Control Consortium and NSF through Grant #CTS-0105360. All simulations and calculations were performed using Octave (http://www.octave.org). Octave is freely distributed under the terms of the GNU General Public License.

Received for review July 1, 2003.

OP0340917